© 1980 The Chemical Society of Japan *Bull. Chem. Soc. Jpn.*, *53*, *854—859 (1980)* [Vol. 53, No. 4

Kinetics of the Gas-phase Photochlorination of Dichloromethane in a Tubular Photoreactor[†]

Takuo SUGAWARA,* Makoto SUZUKI, and Hiroyasu OHASHI
Department of Fuel Chemistry, Mining College, Akita University, Akita 010

(Received July 23, 1979)

The gas-phase photochlorination of dichloromethane was conducted at a low extent of conversion from 9 °C to 100 °C in a tubular flow reactor irradiated by means of a circular array of low-pressure mercury lamps. The kinetics were studied with due consideration taken of the radial variation in light intensity across the reactor and with the proper selection of kinetic equations, including the recombination of dichloromethyl radicals as the dominant termination step. The dependence of the absorbed radiant energy on the chlorine concentration was well simulated by the use of the radial-light and line-source model. The predominance of the observed production rate of hydrogen chloride over that of chloroform was also reproduced well by the appropriately selected kinetic expressions, without any use of the long-chain approximation. The recombination rate constant of dichloromethyl radicals was determined to be $10^{13.5}$ cm^3 mol^{-1} s^{-1}; this is larger than the previously reported value by the factor of 12.6, and is in fair agreement with the theoretical value, $10^{13.3-13.4}$, calculated from the statistical factor, and with the collision rate constant based on the hard-sphere model.

Information has been accumulating for the past two decades on design procedures for photoreactors. The reaction characteristics were examined for a simple kinetic system, combined with the effects of the diffusion rates, the velocity distribution in a flow reactor, and the internal light filtered by a product or by an intermediate.[1,2] However, little work has been reported on photoreactor performance for a reaction system with a complex mechanism. Sugawara *et al.*[3] recently studied the photochlorination of chloroform in an annular reactor. They indicated the necessity for precise information on the kinetics as well as the incident light intensity, especially in the case of a high radiation intensity. Now that research on the angle characteristics of radiation from various types of light sources[4,5] has made possible kinetic studies by the use of a high-intensity lamp in an arbitrary position, it could be possible to examine the effect of a termination step on the overall rates of a reaction with a chain mechanism more precisely than with previous conventional approaches.[6,7]

The motivation of this study was mainly to investigate photoreactor performance in a flow system for series-parallel reactions. First of all, the authors studied the kinetics of the gas-phase photochlorination of dichloromethane in a tubular reactor within a circle of low-pressure mercury lamps. They then discussed the applicability of the long-chain approximation and determined the rate of the recombination of dichloromethyl radicals, one of the termination steps, using the radial-light and line-source model[4] to estimate the radial intensity distribution. The determined rate constant may also be used to estimate the behavior of such air pollutants as dichloromethane and chloroform in the atmosphere.

Stoichiometry and Reaction Mechanism

The stoichiometric equations for the gas-phase photochlorination of dichloromethane are given by Eqs. 1—4, while the proposed reaction mechanisms are given from Eq. 5 through Eq. 17:

$$\mathrm{Cl_2 + CH_2Cl_2 = CHCl_3 + HCl} \tag{1}$$

$$\mathrm{Cl_2 + 2CH_2Cl_2 = C_2H_2Cl_4 + 2HCl} \tag{2}$$

$$\mathrm{Cl_2 + CHCl_3 = CCl_4 + HCl} \tag{3}$$

$$\mathrm{Cl_2 + 2CHCl_3 = C_2Cl_6 + 2HCl} \tag{4}$$

Initiation:

$$\mathrm{Cl_2} \xrightarrow{\phi I_a} \mathrm{2Cl\cdot} \tag{5}$$

Propagation:

$$\mathrm{Cl\cdot + CH_2Cl_2} \underset{k_3}{\overset{k_2}{\rightleftarrows}} \mathrm{CHCl_2\cdot + HCl} \tag{6}$$

$$\mathrm{CHCl_2\cdot + Cl_2} \underset{k_5}{\overset{k_4}{\rightleftarrows}} \mathrm{Cl\cdot + CHCl_3} \tag{7}$$

$$\mathrm{Cl\cdot + CHCl_3} \underset{k_7}{\overset{k_6}{\rightleftarrows}} \mathrm{CCl_3\cdot + HCl} \tag{8}$$

$$\mathrm{CCl_3\cdot + Cl_2} \underset{k_9}{\overset{k_8}{\rightleftarrows}} \mathrm{Cl\cdot + CCl_4} \tag{9}$$

Termination:

$$\mathrm{CHCl_2\cdot + Cl\cdot} \xrightarrow{k_{10}} \mathrm{CHCl_3} \tag{10}$$

$$\mathrm{CHCl_2\cdot + CHCl_2\cdot} \xrightarrow{k_{11}} \mathrm{C_2H_2Cl_4} \tag{11}$$

$$\mathrm{CCl_3\cdot + Cl\cdot} \xrightarrow{k_{12}} \mathrm{CCl_4} \tag{12}$$

$$\mathrm{CCl_3\cdot + CCl_3\cdot} \xrightarrow{k_{13}} \mathrm{C_2Cl_6} \tag{13}$$

$$\mathrm{CHCl_2\cdot + CCl_3\cdot} \xrightarrow{k_{14}} \mathrm{C_2HCl_5} \tag{14}$$

$$\mathrm{Cl\cdot + Cl_2} \underset{k_{16}}{\overset{k_{15}}{\rightleftarrows}} \mathrm{Cl_3\cdot} \tag{15}$$

$$\mathrm{Cl_3\cdot + Cl\cdot} \xrightarrow{k_{17}} \mathrm{2Cl_2} \tag{16}$$

$$\mathrm{Cl\cdot + wall} \xrightarrow{k_{18}} \frac{1}{2}\mathrm{Cl_2} \tag{17}$$

The rate constants recommended in the literature are shown in Table 1.[7-11] The published value of k_{11}, $10^{12.4}$, may be open to question, since it is much lower than k_{13}; a simple kinetic model study[12] suggests that the recombination rate of dichloromethyl radicals should not deviate so much from that of trichloromethyl radicals.

[†] Presented at the Akita Meeting of the Society of Chemical Engineers, Japan, Akita, August, 1974.

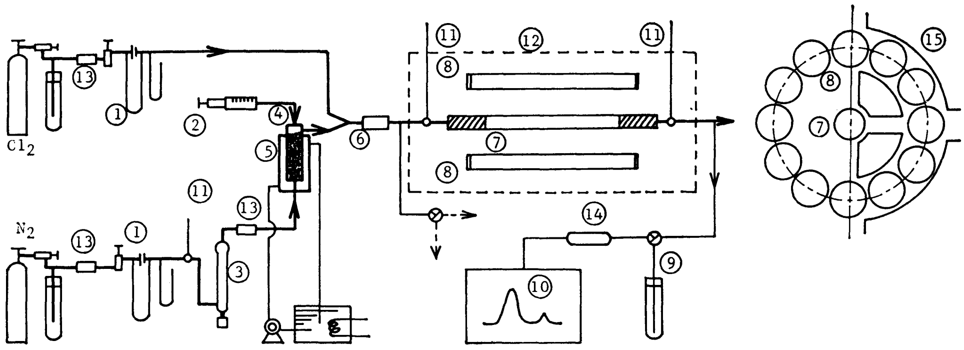

Fig. 1. Schematic diagram of experimental apparatus.
① Orifice meter, ② Microfeeder, ③ Soap-film flow meter, ④ Vaporizer, ⑤ Hot water jacket, ⑥ Mixer, ⑦ Quartz reactor, ⑧ Low pressure mercury lamp, ⑨ KI solution, ⑩ Gas chromatograph, ⑪ Thermometer, ⑫ Air bath, ⑬ Desiccating tube, ⑭ Cl_2 adsorber, ⑮ Bakelite holder.

Table 1. RATE CONSTANTS IN THE LITERATURE FOR THE ELEMENTARY STEPS OF THE PHOTOCHLORINATION OF DICHLOROMETHANE[a)]

$k_2 = 10^{13.4}\exp(-3.10\times10^3/RT)$
$k_3 = 10^{12.0}\exp(-11.2\times10^3/RT)$
$k_4 = 10^{12.0}\exp(-4.00\times10^3/RT)$
$k_5 = 10^{14.0}\exp(-21.0\times10^3/RT)$
$k_6 = 10^{12.8}\exp(-3.35\times10^3/RT)$
$k_7 = 10^{11.7}\exp(-11.3\times10^3/RT)$
$k_8 = 10^{11.7}\exp(-5.00\times10^3/RT)$
$k_9 = 10^{13.9}\exp(-20.0\times10^3/RT)$
$k_{10} = 10^{14.4}$
$k_{11} = 10^{12.4}$
$k_{12} = 10^{13.8}$
$k_{13} = 10^{13.0}$
$k_{14} = 10^{12.1}$
$k_{15} = 4.55\times10^7$
$k_{16} = 7.6\times10^5$
$k_{17} = 1.7\times10^{14}$
$k_{18} = 0.35$

a) R is 1.987 $\mathrm{cal_{th}\ mol^{-1}\ K^{-1}}$, and T is the absolute temperature. k_{12}—k_{15} and k_{17} are in $\mathrm{cm^3\ mol^{-1}\ s^{-1}}$; k_{16} and k_{18} in $\mathrm{s^{-1}}$.

Experimental

Reagents. *Dichloromethane*: The reagent on the market contains ca. 0.5% ethanol as a stabilizer. It produces acetyl chloride and hydrogen chloride by means of this stoichiometric equation (Eq. 18):

$$C_2H_5OH + 2Cl_2 = CH_3COCl + 3HCl \qquad (18)$$

Since the rate of the above reaction was observed in a preliminary study to be much faster than that of the photochlorination of dichloromethane, the ethanol was removed by shaking the mixture with a concentrated sulfuric acid solution and then with a dilute sodium hydroxide solution, followed by distilled water, and finally by drying it with calcium chloride. The remaining dichloromethane was further purified by distillation.

Chlorine and Nitrogen: The effect of the oxygen impurities in chlorine and nitrogen on the photochlorination of dichloromethane was considered negligible because of their extremely small amounts, *i.e.*, several ppm in each cylinder.

Experimental Apparatus and Procedure. A schematic diagram of the apparatus is shown in Fig. 1. Dichloromethane, fed in constantly with a microfeeder (2), was instantaneously vaporized in a vaporizer (4), diluted with nitrogen, and mixed with chlorine in the mixing chamber (6). The reactant gas mixture was then led to a quartz tube (7) through a connecting tube with an inside diameter of 8 mm and a length of 4.5 m. The reactants were irradiated in a test section located *ca.* 15—30 cm downstream from the inlet by means of 3, 6, or 12 low-pressure mercury lamps (Toshiba GL-30, 200 V-30 W; illuminating length, *ca.* 890 mm) arranged in a circle as is shown in the figure. The 100 Hz fluctuation of the light intensity, when the 50 Hz alternating

Table 2. EXPERIMENTAL CONDITIONS

Diameter of reactor, d or $2r_0$/cm	0.588, 0.690
Test-section length, l/cm	18.6, 24.0
Temperature, θ/°C[a)]	9, 58, 100
Total pressure, p/atm[b)]	*ca.* 1
Cl_2concentration, $[Cl_2]/\mathrm{mol\ cm^{-3}}$	$(0.87—2.22)\times10^{-5}$
CH_2Cl_2concentration, $[CH_2Cl_2]/\mathrm{mol\ cm^{-3}}$	$(2.26—4.00)\times10^{-6}$

a) θ/°C$=T$/K-273.15. b) 1 atm$=$101.325 kPa

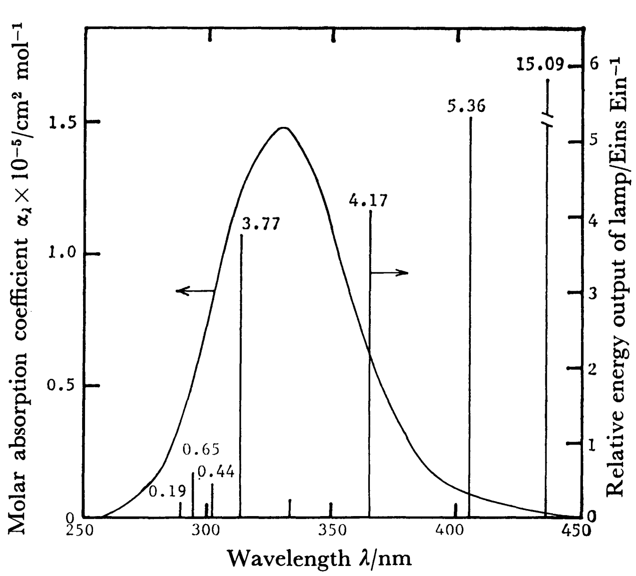

Fig. 2. Spectral distribution of molar absorption coefficient of chlorine and relative energy output of lamp.

current was applied, was minimized by setting one-third of the total number of lamps separately from the three-phase alternating current. The reactor dimensions are summarized in Table 2.

The spectral distribution of the molar absorption coefficient of chlorine,[13] α_λ, is shown in Fig. 2, along with the radiant emission spectra effective for the photochlorination.[14]

Quantitative Analysis. Gas sampled at the reactor inlet or outlet was led into a potassium iodide solution (9) which had been made slightly acidic with hydrochloric acid. The unreacted chlorine and the formed hydrogen chloride were determined with 0.1 mol dm^{-3} sodium thiosulfate and 0.01 mol dm^{-3} sodium hydroxide solutions respectively. Gas sampled through a packed column (14) to be described below was analyzed for dichloromethane, chloroform, and carbon tetrachloride by means of gas chromatography. The column (14) for the adsorption of chlorine was made of a glass tube with an inner diameter of 6 mm and a length of 300 mm, packed with small pellets containing calcium hydroxide, potassium iodide, and calcium chloride. It was ascertained beforehand that the adsorption of the other reactant and products was negligible within the limits of precision of the analysis. A gas chromatograph equipped with a copper column with an inner diameter of 3 mm and a length of 2.2 m, and packed with T.C.P. 30%/celite 545 (80—100 mesh), was operated at 88 °C and at a flow rate of 28.5 cm^3 (20 °C, with 1 atm) min^{-1} of hydrogen as the carrier gas.

Experimental Conditions. All the experiments were conducted under conditions in which a differential reactor could be assumed, where the extent of the conversion of chlorine and dichloromethane was low and where the production of carbon tetrachloride was negligible. The experimental conditions are shown in Table 2. The dark reactions were negligible under the conditions studied.

Results

Incident Light Intensity. It was previously reported that the incident light intensity got lower as time elapsed because of deposits on the reactor wall in the gas-phase photochlorination of hydrocarbons.[8,11,15] A study with a potassium trioxalatoferrate(III) actinometer[16] revealed a gradual drop in intensity, especially during the initial period of usage, but the rate of drop was so slow after about ten hours that the intensity in a run could be considered constant for several hours.

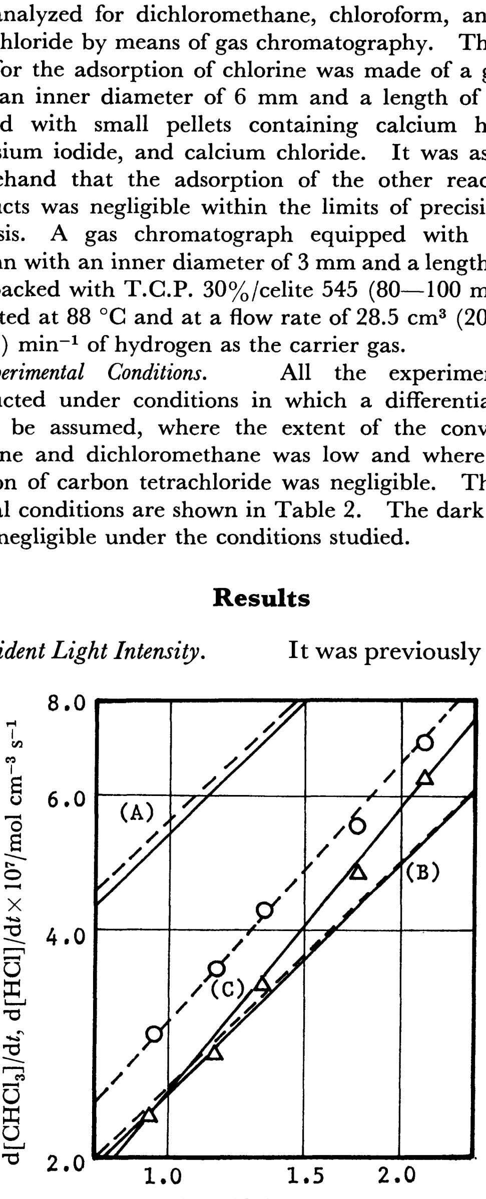

Fig. 3. Formation rates of CHCl$_3$ and HCl.
Exptl. values; △, d[CHCl$_3$]/dt and ○, d[HCl]/dt.
Exptl. conditions; θ/°C=9, d/cm=0.690, l/cm=24.0, [CH$_2$Cl$_2$]/mol cm^{-3}=3.50×10^{-6}, and $(l/\bar{u})$/s=0.465.
Calcd curves; ——, d[CHCl$_3$]/dt and ----, d[HCl]/dt where $\phi\bar{I}_{a,s}\times 10^8$/mol cm^{-3} s^{-1} and k_{11}/cm^3 mol^{-1} s^{-1} are 3.50 and $10^{12.4}$ for (A), 0.75 and $10^{12.4}$ for (B), and 3.50 and $10^{13.5}$ for (C), respectively.

Production Rates of Hydrogen Chloride and Chloroform. Figures 3 and 4 show examples of the effect of the chlorine concentration, and Fig. 5 that of the dichloromethane concentration on the production rates of hydrogen chloride, ○, and chloroform, △. These figures indicate that the effect of chlorine is much greater than that of dichloromethane. The effect of the tempera-

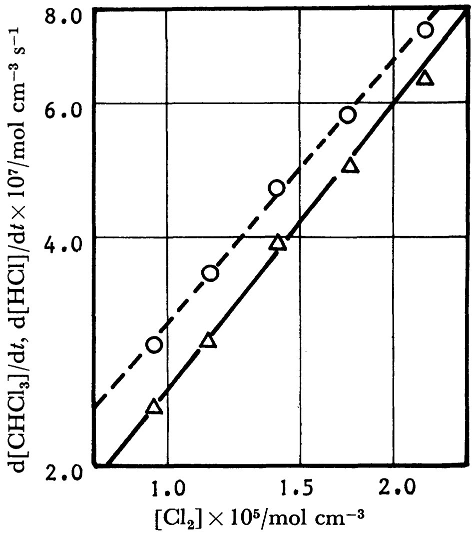

Fig. 4. Effect of chlorine concentration on the formation rates of CHCl$_3$ and HCl.
Exptl. values; △, d[CHCl$_3$]/dt and ○, d[HCl]/dt.
Exptl. conditions; θ/°C=9, d/cm=0.690, l/cm=24.0, [CH$_2$Cl$_2$]/mol cm^{-3}=4.00×10^{-6}, and $(l/\bar{u})$/s=0.534.
Calcd curves; ——, d[CHCl$_3$]/dt and ----, d[HCl]/dt.

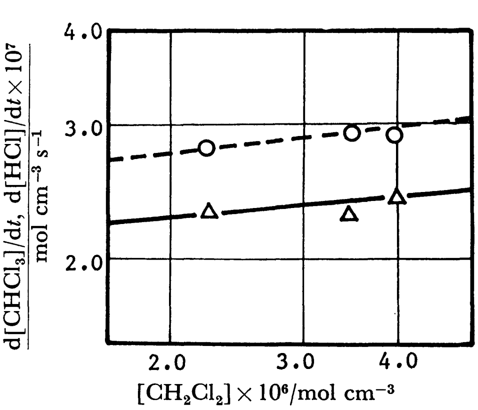

Fig. 5. Effect of dichloromethane concentration on the formation rates of CHCl$_3$ and HCl.
Exptl. values; △, d[CHCl$_3$]/dt and ○, d[HCl]/dt.
Exptl. conditions; θ/°C=9, d/cm=0.690, l/cm=24.0, [Cl$_2$]/mol cm^{-3}=9.60×10^{-6}, and $(l/\bar{u})$/s=0.465–0.534.
Calcd curves; ——, d[CHCl$_3$]/dt and ----, d[HCl]/dt.

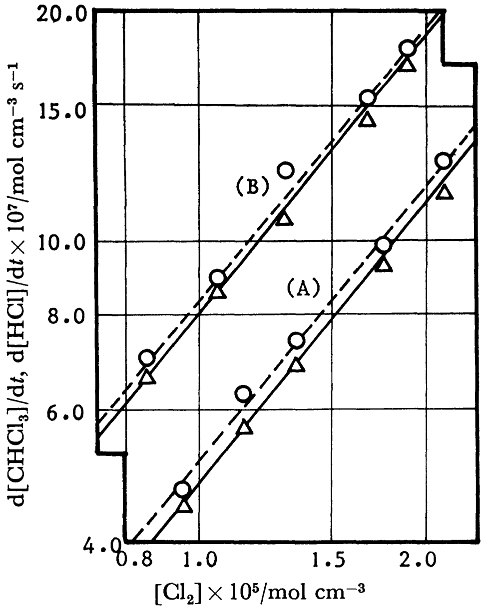

Fig. 6. Effect of temperature on the formation rates of $CHCl_3$ and HCl.
Exptl. values; △, $d[CHCl_3]/dt$ and ○, $d[HCl]dt\cdot/$ Exptl. conditions; $\theta/°C=58$(A) and 100(B), $d/cm=0.588$, $l/cm=18.6$, $[CH_2Cl_2]\times 10^6/mol\ cm^{-3}=3.39$(A) and 3.89(B), and $(l/\bar{u})/s=0.254$(A) and 0.225(B). Calcd curves; ——, $d[CHCl_3]/dt$ and ----, $d[HCl]/dt$.

ture is shown in Fig. 6. Figures 3—6 show that the production rates of hydrogen chloride are higher than that of chloroform, especially at low temperatures.

Discussion

Kinetics under the Conditions of a Low Extent of Conversion. Practical kinetic expressions should be derived to simulate the experimental results, since the proposed reaction mechanism is too complex. First, Eqs. 8, 9 and 12—14 may be neglected, because the chloroform produced was in a low concentration and no appreciable carbon tetrachloride was observed under the experimental conditions studied. Second, back reactions for Eqs. 6 and 7 are insignificant since k_3 and k_5 are much smaller than k_2 and k_4 respectively, as may be seen in Table 1. Third, the concentrations of the chlorine atom and the dichloromethyl radical, calculated by means of Eqs. 6, 7, and 10, and the observed formation rates of hydrogen chloride and chloroform revealed that the effect of Eqs. 15—17 on the total formation rate of chlorine atom is less important than that of Eqs. 6, 7, and 10, in which the trichloro-radical concentration could safely be estimated from the stationary-state hypothesis according to the method of Hutton and Wright.[10]

According to the above discussion, the following kinetic expressions may be considered to be reasonable under the experimental conditions studied:

$$\text{Initiation:}\quad Cl_2 \xrightarrow{\phi I_a} 2Cl\cdot \tag{5}$$

$$\text{Propagation:}\quad Cl\cdot + CH_2Cl_2 \xrightarrow{k_2} CHCl_2\cdot + HCl \tag{19}$$

$$CHCl_2\cdot + Cl_2 \xrightarrow{k_4} Cl\cdot + CHCl_3 \tag{20}$$

$$\text{Termination:}\quad CHCl_2\cdot + Cl\cdot \xrightarrow{k_{10}} CHCl_3 \tag{10}$$

$$CHCl_2\cdot + CHCl_2\cdot \xrightarrow{k_{11}} C_2H_2Cl_4 \tag{11}$$

The production rates of chloroform and hydrogen chloride are represented by Eqs. 21 and 22.

$$\frac{d[CHCl_3]}{dt} = k_4'[CHCl_2\cdot] + k_{10}[Cl\cdot][CHCl_2\cdot] \tag{21}$$

$$\frac{d[HCl]}{dt} = -\frac{d[CH_2Cl_2]}{dt} = k_2'[Cl\cdot] \tag{22}$$

where

$$k_2' = k_2[CH_2Cl_2] \simeq k_2[CH_2Cl_2]_o,$$
$$\text{and}\quad k_4' = k_4[Cl_2] \simeq k_4[Cl_2]_o, \tag{23}$$

and where the subscript o indicates the value at the reactor inlet.

$[Cl\cdot]$ and $[CHCl_2\cdot]$ are obtained by solving Eqs. 24 and 25:

$$\frac{d[Cl\cdot]}{dt} = 2\phi\bar{I}_a - k_2'[Cl\cdot] + k_4'[CHCl_2\cdot] - k_{10}[Cl\cdot][CHCl_2\cdot] \tag{24}$$

$$\frac{d[CHCl_2\cdot]}{dt} = k_2'[Cl\cdot] - k_4'[CHCl_2\cdot] - k_{10}[Cl\cdot][CHCl_2\cdot] - 2k_{11}[CHCl_2\cdot]^2 \tag{25}$$

If the long-chain approximation is applicable, Eq. 26 is obtained for the prediction of the production rates of both chloroform and hydrogen chloride:

$$\frac{d[CHCl_3]}{dt} = \frac{d[HCl]}{dt} = \frac{(\phi\bar{I}_a)^{1/2}k_4[Cl_2]}{\{(k_4k_{10}[Cl_2]/k_2[CH_2Cl_2])+k_{11}\}^{1/2}} \tag{26}$$

Since some difference was observed in the production rates of chloroform and hydrogen chloride, simulation was conducted without the use of the long-chain approximation.

Radial Distribution of Light Intensity in the Reactor. It is necessary to know the relation of the radiant energy absorbed to the chlorine concentration if we are to determine the dependence of the rate of the initiation step on the chlorine concentration.

Now, it is assumed that the radial variation in the chlorine concentration and the effects of reflection and refraction are negligible, and that Beer's law is valid for the absorption of light at each wavelength. Then the light intensity at an arbitrary point P, $I_\lambda(r,\beta)$, and the total energy absorbed, $\bar{I}_a$, are given by Eqs. 27 and 28 respectively when the radial-light and line-source model[4] is applied:

$$I_\lambda(r,\beta) \propto \sum_{j=1}^{n}\left\{\frac{1}{\overline{PO_j}}\exp(-\alpha_\lambda[Cl_2]\overline{PQ_j})\right\} \tag{27}$$

$$\bar{I}_a = \sum_\lambda I_{a,\lambda} \tag{28}$$

where

$$I_{a,\lambda} = \frac{\alpha_\lambda[Cl_2]}{\pi r_o^2}\int_0^{r_o}\int_0^{2\pi} rI_\lambda(r,\beta)d\beta dr \tag{29}$$

$$\overline{PO_j} = (l_o^2+r^2-2l_or\cos\beta_j)^{1/2} \tag{30}$$

$$\overline{PQ_j} = r\cos\alpha_j + (r_o{}^2 - r^2\sin^2\alpha_j)^{1/2} \tag{31}$$

$$\alpha_j = \sin^{-1}[\sin^2\beta_j/\{1+(r/l_o)^2 - 2(r/l_o)\cos\beta_j\}]^{1/2} \tag{32}$$

$$\beta_j = \beta - 2\pi(j-1)/n \tag{33}$$

Symbols refer to Fig. 7.

Figures 8 and 9 show examples of the computed results. The relative radiant energy absorbed, $I_a/I_{a,s}$,[††] as is shown in Fig. 9, was used for the estimation of I_a.

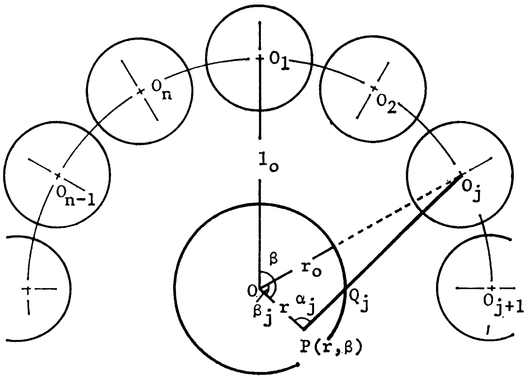

Fig. 7. Arrangement of a reactor and lamps.

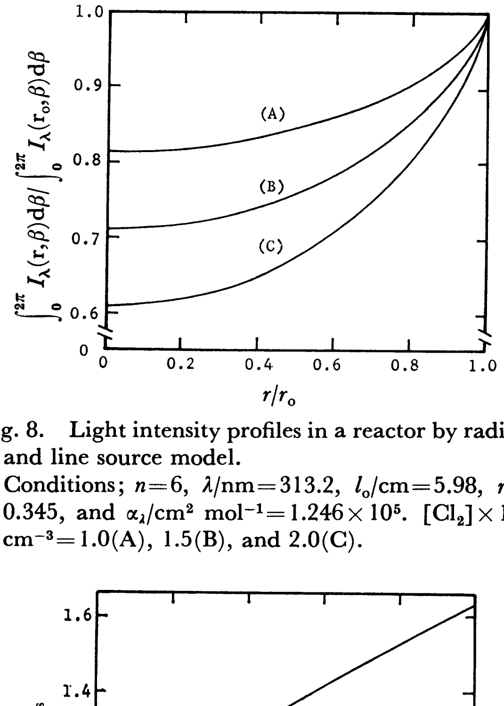

Fig. 8. Light intensity profiles in a reactor by radial light and line source model.
Conditions; $n=6$, λ/nm$=313.2$, l_o/cm$=5.98$, r_o/cm$=0.345$, and α_λ/cm^2 mol^{-1}$=1.246\times10^5$. [Cl$_2$]$\times10^5$/mol cm^{-3}$=1.0$(A), 1.5(B), and 2.0(C).

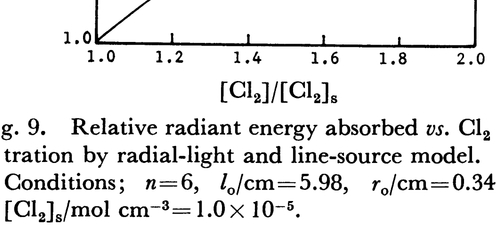

Fig. 9. Relative radiant energy absorbed *vs.* Cl$_2$ concentration by radial-light and line-source model.
Conditions; $n=6$, l_o/cm$=5.98$, r_o/cm$=0.345$, and [Cl$_2$]$_s$/mol cm^{-3}$=1.0\times10^{-5}$.

The procedure will be described in the following section. Funayama *et al.*[5] showed that the radial-light and line-source model was applicable when the distance between a reactor and a low-pressure mercury lamp was less than one-fourth and more than one-eleventh of the lamp length. Thus, we may assume the radial light and line source for the geometric relation in this study.

Determination of the Rate Constant, k_{11}. Assuming no appreciable radial concentration gradient for any reactant, Eqs. 21 and 22 were used to simulate the experimental results. The steady-state chlorine-atom and dichloromethyl-radical concentrations were computed by means of Eqs. 24 and 25, and then applied to Eqs. 21 and 22. The RKG algorithm was used for the computation with the FACOM 270/20, throughout which the quantum efficiency, ϕ, was assumed to be constant. The preliminary study of the parametric sensitivity revealed that $\phi I_{a,s}$ and k_{11} affected the absolute and relative values of the production rates of chloroform and hydrogen chloride respectively when k_2 and k_4 were fixed so as to be correct. It should be noted that k_{10} was less effective than k_{11} for Eqs. 24 and 25, since the chlorine-atom concentration was calculated to be much lower than the dichloromethyl-radical concentration under the conditions studied. I_a for any chlorine concentration was estimated with the relative radiant energy absorbed, $I_a/I_{a,s}$, calculated in the above section, and with an appropriately selected value of $I_{a,s}$ so as to fit the experimental value of the production rate of *chloroform* at a chlorine concentration of 1.0×10^{-5} mol cm^{-3}. Then, the rate constant of the recombination of dichloromethyl radicals, k_{11}, was the parameter to be determined for the estimation of the experimental values of the production rate of *hydrogen chloride*. An example of the simulation is shown in Fig. 3. The solid and the broken lines represent the computed production rates of chloroform and hydrogen chloride respectively, with three sets of $\phi I_{a,s}$ and k_{11}. Although the dependence of ϕI_a on the chlorine concentration was fairly well simulated, the experimental results were not reproduced well for the cases of (A) and (B) in the figure where the previously reported value[8] of k_{11}, $10^{12.4}$, was adopted. Therefore, we sought to optimize k_{11} with an appropriately selected value of $\phi I_{a,s}$.

The experimental data were well simulated when $\phi I_{a,s}$ was assigned a value of 3.50×10^{-8} mol cm^{-3} s^{-1} and when the value of the rate constant, k_{11}, was chosen as $10^{13.5}$ cm^3 mol^{-1} s^{-1}, as is seen in the case of (C) in Fig. 3. The curves thus determined are shown in Figs. 4, 5, and 6, along with the specified values of $\phi I_{a,s}$ and k_{11} and the relative radiant energy absorbed, estimated by means of the radial-light and line-source model. The agreement between the computed and observed values is good, irrespective of changes in the chlorine and dichloromethane concentrations and in the reaction temperature from 9 °C to 100 °C. The good simulation while changing the reaction temperature indicates the reliability of the temperature dependence of the rate constants of the propagation steps and no appreciable activation energy for k_{11}. The determined value of k_{11},

---

[††] The subscript s means the value at the reference concentration, [Cl$_2$]/mol cm^{-3}$=1.0\times10^{-5}$.

$10^{13.5}$, is in fair agreement with the theoretical ones, $10^{13.3}$ at 9 °C and $10^{13.4}$ at 100 °C, calculated from the statistical factor and the collision-rate constant based on the hard-sphere model.12) The radius of the dichloromethyl radical was assumed to be equal to that of dichloromethane17) in the calculation of the collision-rate constant.

Conclusion

For basic information on flow-reactor performance for photoreactions with complex mechanisms, the gas-phase photochlorination of dichloromethane was kinetically studied at a low extent of conversion (from 9 °C to 100 °C) in a tubular quartz reactor irradiated by a circular array of low-pressure mercury lamps. The intense irradiation made it possible to examine the effect of the termination step, the recombination of dichloromethyl radicals, on the overall reaction rate more precisely than with conventional techniques.

The dependence of the absorbed radiant energy on the chlorine concentration was well simulated by the radial-light and line-source model, which takes the radial-intensity variation into consideration. The predominance of the observed production rate of hydrogen chloride over that of chloroform was also reproduced well by the appropriately selected kinetic equations without any use of the long-chain approximation.

The recombination-rate constant of the dichloromethyl radicals was determined to be $10^{13.5}$ cm^3 mol^{-1} s^{-1}. No appreciable activation energy was observed in the temperature range from 9 °C to 100 °C. The determined value is larger than the previously reported one by a factor of 12.6, and it is in fair agreement with the theoretical one, $10^{13.3-13.4}$, calculated from the statistical factor and the collision-rate constant based on the hard-sphere model.

This paper was prepared when one of the authors (T.S.) was at the University of Minnesota. Professor R. W. Carr's comments are appreciated. The authors also appreciate the experimental assistance of Mr. Hajime Muto. This work was supported by a Grant-in-Aid for Scientific Research from the Ministry of Education, Japan, in 1973 (No. 875485).

References

1) T. Sugawara, K. Omori, and H. Ohashi, *Kagaku Kogaku Ronbunshu*, **2**, 304 (1976).

2) T. Sugawara, K. Omori, and H. Ohashi, *J. Chem. Eng. Jpn.*, **12**, 143 (1979).

3) T. Sugawara, H. Ohashi, and T. Tadaki, *Kagaku Kogaku Ronbunshu*, **1**, 160 (1975).

4) T. Akehata and T. Shirai, *J. Chem. Eng. Jpn.*, **5**, 385 (1972).

5) H. Funayama, K. Ogiwara, T. Sugawara, and H. Ohashi, *Kagaku Kogaku Ronbunshu*, **3**, 354 (1977).

6) J. M. Tedder and J. C. Walton, *Trans. Faraday Soc.*, **63**, 2426 (1967).

7) G. R. De Maré and G. Huybrechts, *Trans. Faraday Soc.*, **64**, 1311 (1968).

8) G. Chiltz, P. Goldfinger, G. Huybrechts, G. Martens, and G. Verbeke, *Chem. Rev.*, **63**, 355 (1963).

9) R. Eckling, P. Goldfinger, G. Huybrechts, G. Martens, and G. Verbeke, *Chem. Ber.*, **93**, 3014 (1960).

10) E. Hutton and M. Wright, *Trans. Faraday Soc.*, **61**, 78 (1965).

11) T. Sugawara, T. Tadaki, and S. Maeda, *Kagaku Kogaku*, **37**, 614 (1973). The treatment is reviewed in "Hanno Sokudo no Kogaku," The Society of Chem. Eng. Jpn., Maruzen, Tokyo (1974), pp. 179—180.

12) R. E. Weston, Jr., and H. A. Schwarz, "Chemical Kinetics," Prentice-Hall, Englewood Cliffs (1972), pp. 89—90.

13) H. V. Halban and K. Seidentopf, *Z. Phys. Chem.*, **103**, 71 (1922).

14) "Toshiba Review," Toshiba, Tokyo (1956), Vol. 11, No. 9, p. 1019.

15) D. Ziolkowski, A. E. Cassano, and J. M. Smith, *AIChE J.*, **13**, 1025 (1967).

16) C. A. Parker, *Proc. R. Soc. London. Ser. A*, **220**, 104 (1953).

17) R. B. Bird, W. E. Stuart, and E. N. Lightfoot, "Transport Phenomena," John Wiley and Sons, New York (1960), p. 745.